Textile & Leather Review

ISSN 2623-6281| www.tlr-journal.com | 10.31881/TLR

A Unified Analytical Framework for Dynamically Stable and Energy-Efficient Motion Planning in Humanoid Robots

Junning Fu

How to cite: Fu J. A Unified Analytical Framework for Dynamically Stable and Energy-Efficient Motion Planning in Humanoid Robots. Textile & Leather Review. 2026; 9:2146-2169. https://doi.org/10.31881/TLR.2026.2146

How to link: https://doi.org/10.31881/TLR.2026.2146

Published: 25 April 2026

A Unified Analytical Framework for Dynamically Stable and Energy-Efficient Motion Planning in Humanoid Robots

Junning Fu

Tianyou College, East China Jiaotong University, Nanchang 330013, China

CenchersFu331@outlook.com

Article

https://doi.org/10.31881/TLR.2026.2146

Published 25 April 2026

ABSTRACT

With the increasing complexity of tasks assigned to humanoid robots, planning dynamically stable and energy-efficient motions remains a significant challenge. This study addresses the problem of generating collaborative, multi-joint movements for humanoid robots, exemplified by a complex dance performance representing the coordinated limb movements required in advanced garment manufacturing, while simultaneously ensuring stability and optimizing energy consumption. We propose a unified analytical framework that combines precise kinematic modeling with integrated stability control. The methodology employs Homogeneous Transformation Matrices (HTM) for accurate end-effector positioning and motor torque validation. C^2-continuous 5th-order polynomial interpolation is utilized for trajectory generation to ensure smoothness and minimize jerk. Critically, we integrate the Zero-Moment Point (ZMP) stability criterion directly into the motion planning phase, enabling proactive leg adjustments to compensate for upper-body dynamics. This integrated model facilitates the analytical calculation of total energy consumption, including motor torque and thermal effects, allowing for subsequent optimization. The significance of this research lies in providing a computationally lightweight, deterministic, and holistic solution for real-time motion planning. It offers a practical alternative to computationally expensive, iterative optimization algorithms, which is essential for the real-time deployment of humanoid platforms in dynamic environments such as smart textile assembly lines.

KEYWORDS

humanoid robots, motion planning, zero-moment point (ZMP), energy optimization, textile automation

INTRODUCTION

The increasing integration of robotics into complex, human-centric environments has propelled the development of advanced motion control systems. Humanoid robots, in particular, offer unparalleled

potential for tasks requiring anthropomorphic interaction and dexterity. However, planning and executing dynamic movements presents a formidable challenge that exists at the intersection of several competing objectives: achieving expressive and complex motions, maintaining dynamic stability to prevent failure, and optimizing energy consumption to ensure operational longevity. Consequently, developing a framework that can holistically and efficiently co-optimize these objectives remains a critical frontier in contemporary robotics research. In the context of the 'Smart Factory', the textile industry increasingly demands humanoid robots capable of handling semi-structured tasks, such as flexible material sorting and garment logistics, which require high dynamic stability during upper-body manipulation.

Current research predominantly tackles this challenge through two primary, yet often separate, methodological pillars. The first pillar is trajectory optimization, which aims to generate optimal motion paths according to specific performance criteria. This process typically begins with foundational kinematic modeling [1,2] and then employs high-order polynomials to generate smooth, C^2-continuous joint trajectories [3-5]. To achieve optimality, a vast body of literature relies on computationally intensive metaheuristic and evolutionary algorithms [6-9]. These techniques are frequently applied within multi-objective optimization frameworks [10-13] to navigate the intricate trade-offs between performance indicators, with a strong focus on minimizing time and energy consumption [14].

The second fundamental pillar is dynamic stability control, which focuses on preventing the robot from falling during motion. Research in this domain has established the Zero-Moment Point (ZMP) criterion as a cornerstone principle for generating stable walking patterns [15] and enabling advanced control strategies through ZMP manipulation [16], even across varied platforms [17] and under sophisticated control schemes like Model Predictive Control (MPC) [18]. Complementary stability concepts, such as the Capture Point, are also utilized to optimize the robot's center of mass motion in real-time [19].

Despite the progress within each pillar, their separation reveals a critical methodological schism that hinders practical application. The trajectory optimization approaches are not only computationally expensive and non-deterministic, rendering them unsuitable for real-time scenarios, but they also tend to oversimplify stability constraints. Conversely, the stability-focused studies often treat the reference trajectory as a pre-determined input, verifying stability post-hoc rather than embedding it as an intrinsic constraint during generation. This decoupling persists even when analytical models are considered for energy minimization [20], as they are rarely integrated a priori with rigorous dynamic stability constraints. This fundamental

separation between planning for optimality and ensuring stability leads to computationally burdensome, suboptimal, and often infeasible motion plans.

To bridge this methodological gap, this paper introduces a unified analytical framework that holistically methodologically integrates dynamic stability and energy optimization within the analytical derivation. Our methodology deliberately avoids the pitfalls of iterative optimization by leveraging a deterministic, analytical approach that is computationally lightweight. We employ Homogeneous Transformation Matrices (HTM) for precise forward kinematic modeling and C^2-continuous 5th-order polynomials for motion smoothness. Most critically, our framework embeds the ZMP stability criterion as a proactive constraint within the trajectory generation phase, enabling the analytical computation of compensatory leg movements to ensure stability a priori. This unified structure then facilitates the direct derivation of total energy consumption, allowing for subsequent optimization without compromising the stability guarantees. We argue that this approach provides a practical and robust alternative, offering an effective solution for planning complex, collaborative movements for humanoid robots in real-time.

THE FUNDAMENTAL MODELING FRAMEWORK

To address the multifaceted challenges in humanoid robot motion planning, we propose an integrated modeling framework comprising two primary, interrelated components. The first part establishes an accurate and verifiable kinematic foundation for single-limb motion, ensuring positional precision and physical safety. The second part builds upon this foundation to construct an integrated, stability-aware model for generating complex multi-joint collaborative motions.

The Structure of the Analytical Forward Kinematics Model

Calculating the final position of an end-effector after specified joint rotations in humanoid robots forms the foundation for all subsequent complex motion planning tasks. To simplify solutions, some models often employ spherical coordinate systems. However, while intuitive, this approach falls short for rigorous robotic applications because it obscures the non-commutativity of three-dimensional rotations and fails to accurately simulate the physical constraints of rigid body systems. Therefore, we propose an analytical forward kinematics model based on rigid body transformation principles, providing a more robust and

physically accurate foundation for research. This model draws inspiration from established geometric approaches in robotics.

The fundamental principle of this model is that the spatial displacement of a rigid body can be described as a sequence of rotations and translations, which are mathematically represented by matrix multiplications. The final orientation and position of a point on the body depend critically on the order of these transformations.

The modeling process begins by defining the robot's arm as a vector in its initial state. A sequence of rotation matrices, corresponding to the specified joint movements, is then applied to this vector. The core kinematic transformation is established as follows:

$$p_{final} = R_z(\gamma)R_y(\beta)p_{initial} \quad (1)$$

where pfinal represents the final 3D position vector of the arm's end-effector, Rz(γ) is the rotation matrix about the Z-axis (yaw) by an angle γ, Ry(β) is the rotation matrix about the Y-axis (pitch) by an angle β, pinitial is the initial 3D position vector of the end-effector, assumed to be L00]T, where L is the length of the arm.

A crucial aspect of this model is the integration of safety verification. The motion is only considered viable if the resulting torque on the actuator remains within its operational limits. The gravitational torque is the primary load in this static scenario.

$$\tau_g = r_{com} \times F_g \quad (2)$$

where τg is the gravitational torque vector exerted at the shoulder joint, rcom is the position vector from the shoulder joint to the arm's center of mass. For a uniform arm, this is pfinal/2,Fg is the gravitational force vector, acting on the arm's CoM, given by 0,0,−mg]T,m is the mass of the arm and g is the acceleration due to gravity. The safety condition is then $|\tau_g| \leq \tau_{max}/S_f$, where τ_{max} is the maximum permissible torque and S_f is a preliminary static safety factor. It is crucial to note that this static verification serves only as a prerequisite screening to eliminate kinematically infeasible postures under gravity. It does not guarantee dynamic safety during high-speed motion; the full dynamic feasibility, accounting for inertial, Coriolis, and

centrifugal terms, is subsequently rigorously verified in the energy optimization model (Section The structure of the Analytical Energy Consumption and Optimization Model) using the Lagrangian dynamics formulation. The mechanism of this model follows a deterministic, sequential process: Firstly, the robot's left arm is modeled as an initial vector pinitial with magnitude equal to the arm length, aligned along the local x-axis. Secondly, a sequence of rotations, as defined by the problem statement, is applied. Corresponding rotation matrices Ry(β) and Rz(γ) are constructed. Thirdly, the final coordinate pfinal is computed by sequentially multiplying the initial vector by the rotation matrices, as shown in Equation (1). This provides the precise Cartesian coordinates of the hand. Subsequently, the model calculates the position of the arm's CoM. Using the final CoM vector and the gravitational force vector, the resulting static torque τg at the shoulder is computed via the cross product in Equation (2). Finally, the magnitude of the calculated torque is compared against the known maximum rated torque of the motor. Consequently, the model not only provides an accurate position but also validates the physical feasibility and safety of the specified posture.

The Structure of the ZMP-Constrained Dynamic Trajectory Generation Model

For the complex multi-joint collaborative motion of humanoid robots, a simple kinematic model is insufficient. Drawing on fundamental ZMP theory and modern advances in stability control, we propose an integrated, feedforward-active model. The ZMP-constrained dynamic trajectory generation model analytically links upper-body motion with necessary lower-body compensatory movements, structurally ensuring stability.

The core principle of this model is the cause-and-effect relationship between body motion, the Center of Mass (CoM) dynamics, and the Zero-Moment Point (ZMP). Any movement of the upper body induces a shift in the robot's total CoM. The acceleration of this CoM, in turn, dictates the position of the ZMP. To maintain balance, the ZMP must always remain within the support polygon formed by the feet. Our model leverages this principle by calculating the ZMP shift caused by the upper body and then synthesizing the required leg motion to maintain stability.

The model is built upon three pillars: analytical trajectory generation for the upper body, ZMP prediction based on CoM dynamics, and a leg compensation mechanism solved via inverse kinematics.

To ensure smoothness and predictability, the upper body trajectory is defined analytically. Body rotation is modeled using a fifth-order polynomial, which guarantees C^2 continuity—an approach supported by recent research on smooth trajectory planning [3-5].

$$\theta_{body}(t) = a_5 t^5 + a_4 t^4 + a_3 t^3 + a_2 t^2 + a_1 t + a_0 \quad (3)$$

where θbody(t) is the body's yaw angle at time t,ai are coefficients determined by boundary conditions (initial and final position, velocity, and acceleration, which are all zero for a smooth start and stop).

The arm's circular motion is described by standard parametric equations:

$$p_{arm}(t) = \begin{bmatrix} x_c \\ y_c + Rcos\,(\omega t + \phi) \\ z_c + Rsin\,(\omega t + \phi) \end{bmatrix} \quad (4)$$

where parm(t) is the position of the hand relative to the shoulder, R is the radius of the circular motion, ω is the angular frequency, and ϕ is the phase offset.

The total CoM of the robot is the mass-weighted average of all its links. **approximating the end-effector geometry as a point mass** the ZMP can be predicted from the CoM trajectory using the simplified cart-table or Linear Inverted Pendulum Model (LIPM) equation, a foundational concept from Kajita et al. [15]: It is important to distinguish that this simplified LIPM is employed solely for the fast, real-time generation of reference trajectories. The subsequent validation and stability verification (discussed in Section Results and analysis) utilize a high-fidelity full multi-body dynamics simulation that includes inertial effects of all links, ensuring that the simplified planning model remains valid under realistic physical constraints.

$$x_{zmp} = x_{com} - \frac{z_{com}}{g} \ddot{x}_{com} \quad (5)$$

where x_{zmp} and x_{com} are the positions of the ZMP and CoM in the x-direction, respectively, $\ddot{x}_{com}$ is the acceleration of the CoM. z_{com} represents the effective operational height of the CoM. While complex motions involve vertical dynamics, for the collaborative gestures focused on in this study, the vertical acceleration $\ddot{z}_{com}$ is negligible compared to gravity (g). Thus, z_{com} is assumed constant to decouple the dynamics and ensure the analytical solvability of the trajectory generation without significant loss of stability

precision. The ZMP position calculated from Equation (5) using the upper-body motion represents the ZMPrequired to perform the movement without external moments. To ensure this required ZMP stays within the support polygon, the robot must shift its entire body. This is achieved by adjusting the legs. The problem becomes finding the leg joint angles, θleg, that position the robot's hips and torso such that the total body CoM produces the desired stable ZMP. This is fundamentally an inverse kinematics problem.

$$\theta_{leg} = IK(p_{hip\_target}) \tag{6}$$

where θleg represents the vector of joint angles for the hip, knee, and ankle. IK is the inverse kinematics solver function. phip_target is the target position of the hip joint in the world frame, calculated to shift the CoM appropriately.

The mechanism of this integrated model operates in a feedforward, analytical cascade:

Upper-Body Planning: At any given time within the performance window [0, 4s], the exact angular position of the main body and the Cartesian coordinates of both hands are calculated analytically using Equations (3) and (4).

CoM and ZMP Derivation: Based on these upper-body trajectories and the robot's mass properties, the trajectory of the total CoM and its second derivative are computed. Using Equation (5), the model then calculates the ZMPrequired trajectory—the path the ZMP must follow on the ground to support the upper-body motion.

Stability Constraint Application: Although this ZMP required is mathematically derived, it may fall outside the physical support polygon, leading to a fall. Therefore, the model's core mechanism is to constrain this ZMPrequired to a safe, central path within the support polygon.

Compensatory Motion Generation: The difference between the ZMP generated by the uncompensated CoM and the desired stable ZMP target informs the necessary corrective shift of the total CoM. This required CoM shift is then translated into a target displacement for the robot's hips.

Inverse Kinematics Solution: Finally, using the target hip position relative to the fixed feet, an inverse kinematics solver (Equation 6) calculates the precise joint angles for the hips, knees, and ankles. This leg

motion actively shifts the lower body to counterbalance the upper body, effectively keeping the ZMP within stable bounds.

Holistic Trajectory Output: Consequently, the model outputs a complete, time-synchronized set of joint angle trajectories for every joint in the robot (torso, arms, and legs) that is guaranteed by its construction to be smooth, C^2-continuous, and dynamically stable. This contrasts sharply with iterative optimization methods [8-9], as it provides a deterministic and computationally lightweight solution.

The Structure of the Analytical Energy Consumption and Optimization Model

With the kinematic and dynamic trajectories established, the final and most critical phase of the modeling process is to quantify and subsequently optimize the energy consumption required to execute these motions. An accurate energy model is not merely an accounting tool; it is the objective function that guides the optimization process. This model moves beyond simple mechanical work, incorporating electrical inefficiencies and thermal losses to provide a holistic view of the power demanded from the robot's battery. This approach is informed by analytical energy modeling principles seen in recent robotics research [20].

The model is constructed on the principle that the total energy consumed is the time integral of the total electrical power drawn by all joint motors. This electrical power is composed of the mechanical power required to move the limbs and overcome gravity, plus the power lost as heat due to motor inefficiencies.

Unlike the static case in section The structure of the Analytical Forward Kinematics Model, dynamic torque is a function of the entire robot's state. We first establish the robot's equation of motion using the Lagrangian formulation

$$\tau(t) = M(\theta)\ddot{\theta} + C(\theta,\dot{\theta})\dot{\theta} + G(\theta) + \tau_{fric}(\dot{\theta}) \quad (7)$$

where τ(t) is the vector of joint torques required at time t. θ(t), $\dot{\theta}$(t), and $\ddot{\theta}$(t) are the vectors of joint angles, velocities, and accelerations, respectively, obtained directly from the analytical trajectories planned in Section The structure of the ZMP-Constrained Dynamic Trajectory Generation Model. M(θ) is the mass-inertia matrix of the robot, which is configuration-dependent. C(θ,$\dot{\theta}$) is the matrix of Coriolis and centrifugal torques.G(θ) is the vector of gravitational torques. $\tau_{fric}(\dot{\theta})$ represents the joint friction torque, modeled as

a combination of Coulomb and viscous friction ($\tau_{fric} = F_v\dot{\theta} + F_c\text{sgn}(\dot{\theta})$) to account for mechanical losses in the gearboxes and bearings, which are significant in humanoid platforms.

The instantaneous mechanical power for a single joint i is the product of its torque and angular velocity. The total mechanical power is the sum over all n joints:

$$P_{mech}(t) = \sum_{i=1}^{n} \tau_i\,(t) \cdot \dot{\theta}_i(t) \tag{8}$$

However, electric motors are not entirely efficient. The electrical power drawn from the battery must account for these losses. The model also considers regenerative braking capability, whereby the mechanical power generated when the load drives the motor can be partially converted back into electrical energy.

$$P_{elec}(t) = \sum_{i=1}^{n} \begin{cases} \frac{P_{mech,i}(t)}{\eta_m} & \text{if } P_{mech,i}(t) \geq 0 (\text{Motoring}) \\ P_{mech,i}(t) \cdot \eta_r & \text{if } P_{mech,i}(t) < 0 (\text{Regenerating}) \end{cases} \tag{9}$$

where Pelec(t) is the total instantaneous electrical power. Pmech, i(t) is the mechanical power of joint i. ηm is the motor efficiency during positive work. ηr is the regenerative efficiency during braking.

A significant portion of energy loss manifests as heat, primarily due to the internal resistance of the motor windings, known as Joule heating. This can be modeled based on the current required to generate the desired torque.

$$\tau_i(t) = K_{t,i} \cdot I_i(t) \Longrightarrow P_{thermal,i}(t) = I_i(t)^2 R_i = \left(\frac{\tau_i(t)}{K_{t,i}}\right)^2 R_i \tag{10}$$

where Pthermal, i(t) is the thermal power dissipated by joint i. Kt,i is the torque constant of the motor i. Ii(t) is the current through the motor i. Ri is the internal resistance of the motor i.

The total energy consumed over a motion of duration T is the integral of the total electrical power. This forms the objective function for our optimization.

$$E_{total} = \int_0^T P_{elec}(t)dt \quad (11)$$

The optimization problem is thus formulated as minimizing Etotal by adjusting the parameters of the trajectory functions defined in Section 2.2, while simultaneously satisfying all kinematic, dynamic, and ZMP stability constraints.

The energy model operates as the final analytical layer of our framework. We identify a set of tunable parameters, α, within our analytical trajectory models from Section The structure of the ZMP-Constrained Dynamic Trajectory Generation Model to serve as the optimization variables. Specifically, the parameter vector is defined as $\alpha = [T, \phi, \omega]^T$, where T denotes the total duration of the motion (which directly scales the polynomial coefficients a_i in Eq. 3), and ϕ, ω represent the phase offset and angular frequency of the arm's parametric motion (Eq. 4), respectively. For a given set of parameters α, the framework first generates the full joint trajectories (θ(t),θ˙(t),θ¨(t)). These trajectories are then fed into the dynamic model (Equation 7) to compute the required joint torques τ(t). Subsequently, the electrical power Pelec(t) is calculated using Equation (9), which accounts for motoring and regenerative efficiencies. The total energy Etotal is computed by integrating Pelec(t) over the motion duration T, as per Equation (11). The core of the optimization mechanism is to find the parameter set α∗ that minimizes Etotal:

$$\alpha^* = arg \min_{\boldsymbol{\alpha}} E_{total}(\alpha) \text{s.t. ZMP} \in \text{Support Polygon} \quad (12)$$

Unlike stochastic methods [8-9], because our entire model is analytical, we can employ efficient gradient-based optimization methods. By computing the partial derivatives ∂Etotal∂αj, we can use algorithms like gradient descent to rapidly converge to a locally optimal, energy-efficient trajectory.

The final output is the set of joint trajectories generated using the optimized parameters α∗. This plan is, by construction, smooth, dynamically stable, and optimized for minimal energy consumption.

Integrated Model Validation and Robustness Analysis Framework

A theoretical model is only valuable if it accurately reflects physical reality. Therefore, we propose a rigorous validation framework to assess the fidelity and robustness of the integrated planning model. This framework

employs high-fidelity simulations and sensitivity analysis to bridge the gap between our analytical derivations and actual performance.

The validation framework is based on a “predict-then-verify” principle and is structured in two stages:

(1) Software-in-the-Loop (SIL) Simulation. This phase tests the direct performance of the planned trajectory in a simulated physical environment.

(2) Sensitivity and Robustness Analysis. This stage probes the model’s resilience to the inevitable uncertainties of the real world, such as modeling errors and parameter drift.

The operational mechanism of this framework is as follows:

(1) Simulation Execution (SIL). The optimized joint angle trajectories $\theta*(t)$ generated by the full framework are used as the reference commands for the joint position controllers of a simulated robot model. This model has its own physics engine, including mass, inertia, friction, and contact dynamics. During the simulation, we continuously record key performance metrics that are not directly commanded, such as the actual ground reaction forces (from which the “true” ZMP can be calculated), the actual CoM trajectory, and the torques applied by the simulated actuators to track the reference trajectory. The analytically-predicted ZMP trajectory is compared to the ZMP trajectory calculated from the simulated ground reaction forces. A close match (low Root Mean Square Error) validates the predictive power of our LIPM-based model (Equation 5) and confirms that the robot remains stable. The analytically-calculated dynamic torques (from Equation 7) are compared with the torques measured from the simulated actuators. A high correlation confirms the accuracy of the identified dynamic parameters (M,C,G).

(2) Robustness Analysis. To test robustness, we introduce controlled uncertainties into the simulation model that were not present in the planning model. For example, we might increase the mass of an arm by 5%, reduce the maximum output torque of a motor by 10%, or add a small, constant external push force. The original, un-modified optimal trajectory is then executed on this new, “imperfect” simulated robot. The key assessment is whether the robot can still complete the task without falling. We monitor the ZMP position during the perturbed simulation. If the ZMP remains within the support polygon despite the unexpected perturbations, the planning model is considered robust. This analysis is crucial because it demonstrates that the stability margins inherent in our planning process are sufficient to handle minor real-world discrepancies, a critical feature for practical deployment.

Consequently, this comprehensive validation process not only confirms the correctness of our proposed models but also quantifies their reliability and resilience in the face of real-world imperfections.

RESULTS AND ANALYSIS

Model simulation will utilize representative parameters of lightweight humanoid robots, consistent with those of Unitree Technology's Unitree G1 series robots.

The data used in this paper is sourced from https://www.unitree.com/cn/gl and https://support.unitree.com/home/zh/G1_developer/about_G1

Results and Analysis of the Analytical Forward Kinematics Model

The Analytical Forward Kinematics Model described in Section The structure of the ZMP-Constrained Dynamic Trajectory Generation Model is used to solve the precise calculation of joint angles and positions for humanoid robots and to verify the safety of their movements.

We construct a scenario: The Unitree G1 robot extends and raises its left arm from its initial position, forming an angle with its body while simultaneously rotating the arm leftward by a certain angle, approximating the end-effector geometry as a point mass. Establishing a Cartesian coordinate system with the robot's shoulder as the origin (0,0,0), the x-axis points directly forward, the y-axis extends horizontally to the robot's left, and the z-axis is perpendicular to the ground and points upward.

Based on the relevant parameters of the Unitree G1, we can calculate the final coordinates of the end effector. The relevant parameters of the Unitree G1 are shown in Table 1.

Table 1. Unitree G1 Robot Specifications

Parameter	Value
arm length (L1)	338 mm
pitch angle (β)	60°
yaw angle (γ)	30°

Assume the mass of the G1 robotic arm, including actuators and structure, is 2.0 kg. This represents a reasonable estimate for a lightweight humanoid arm of this size. Assume the shoulder joint motor has a rated torque of 20.0 Nm. This value reflects the typical level of high-performance motors used in modern humanoid robots such as the Unitree G1, providing a realistic benchmark for safety assessments.

After substituting the data into the model, the final coordinate position of the arm can be determined, and the safety factor is calculated to yield the quantitative results summarized in Table 2. Arm position in three planes is shown in Figure 1.

Table 2. Kinematic and Safety Analysis Results

Parameter	Value
Final X(mm)	146.36
Final Y (mm)	84.50
Final Z (mm)	292.72
Gravitational Torque (Nm)	2.22
Safety Factor	9.01

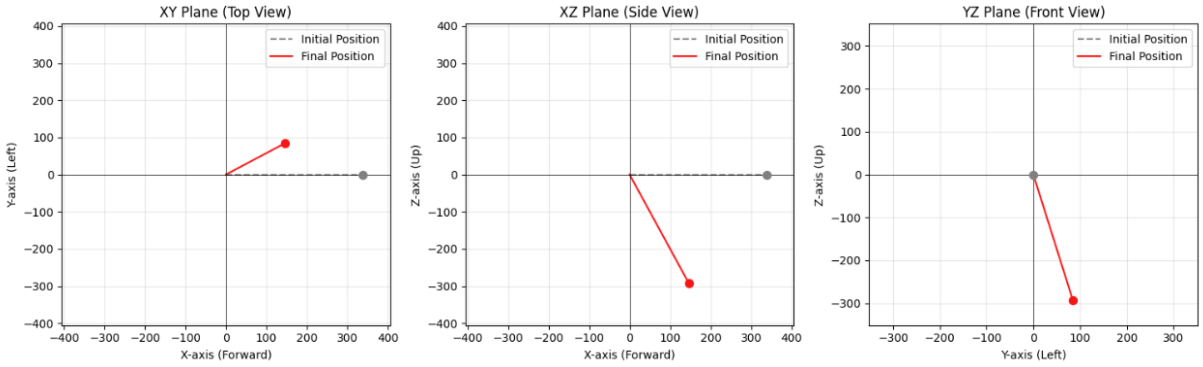

Figure 1. Arm Position in Three Planes

The results clearly indicate that the final position of the end-effector is at coordinates (146.36, 84.50, 292.72) mm relative to the shoulder origin. More importantly, the static gravitational torque exerted on the shoulder joint is calculated to be 2.22 Nm. Given our reasonable assumption of a 20.0 Nm rated torque for the motor, this posture results in a safety factor of 9.01.

A safety factor substantially greater than 1.0 indicates that the motor is operating well within its safe limits. Therefore, we can conclude with high confidence that the specified static posture is both kinematically achievable and physically safe for the robot. Although this analysis is static, it provides a critical baseline. However, for dynamic motions involving acceleration, the required torque will be significantly higher. Consequently, the analysis of dynamic stability and loading, as explored in the next section, is essential.

Results and Analysis of the ZMP-Constrained Dynamic Trajectory Generation Model

For multi-joint collaborative motion planning in robots, the ZMP constraint-based dynamic trajectory generation model can be employed to synthesize whole-body movements. This yields the temporal relationships between the angles of each joint in the humanoid robot's arm and leg segments during specific action sequences that ensure the robot's equilibrium.

Establish the following practical scenario: The Unitree G1 robot first rotates its body to the left by a certain angle while simultaneously performing circular movements with both arms around the shoulders at a specific frequency and radius. The arms move in opposite directions. Throughout the process, the robot must maintain its balance and avoid any loss of stability, such as falling over.

Based on the above scenario, the initial data is shown in Table 3.

Table 3. Initial Data

Parameter	Value
Cycle (s)	4
Yaw Angle Magnitude (°)	45
Radius of circular motion(mm)	300

The total mass of the robot is taken from official specifications as 47kg. The Center of Mass (CoM) height (zcom) is assumed to be 0.8m. The support polygon, formed by the robot's feet, is assumed to be a rectangle with a length (heel-to-toe) of 0.25m and a stance width of 0.20m. This is a representative stance for a bipedal robot of this size.

The simulation yields two critical visualizations. Figure 2 illustrates the compensatory trajectory that the robot's Center of Mass must follow, which is achieved by the leg joints. Figure 3 provides the most crucial result: a comparison of the ZMP trajectory with and without the compensation mechanism.

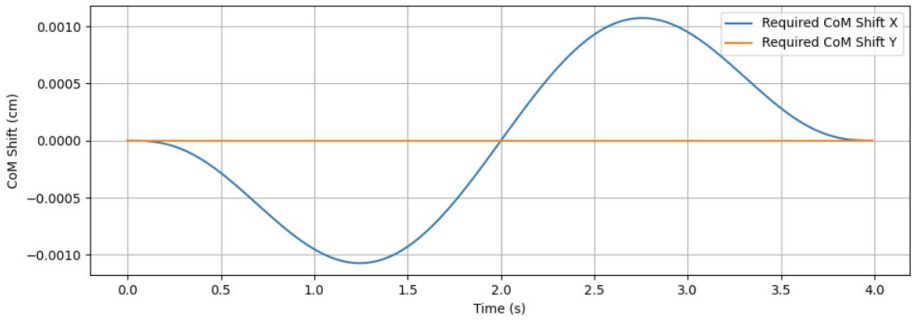

Figure 2. Required Compensatory CoM Trajectory

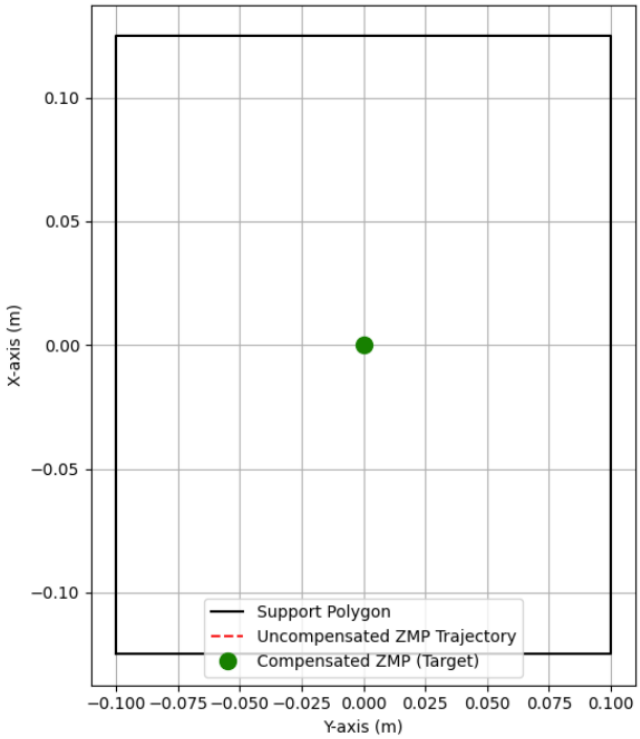

Figure 3. ZMP Stability Analysis

As shown in Figure 3, the uncompensated zero-point trajectory clearly illustrates the robot's behavior when performing only upper-limb movements. The zero-point trajectory would trace a path significantly offset, deviating several meters beyond the support polygon's boundaries. This implies the robot would immediately lose balance and suffer a catastrophic fall.

However, by employing the ZMP constraint model, a compensatory center-of-mass displacement can be calculated, as shown in Figure 2. This displacement, executed by the legs, actively counteracts the effects of the upper-limb movement. The final result is that the actual ZMP remains fixed at the target compensatory ZMP point, which is safely positioned within the center of the support polygon. The required center-of-mass displacement is minimal, on the order of just a few centimeters, indicating that the balancing action will be subtle and highly efficient.

These results powerfully validate the efficacy of the proposed model. It demonstrates that for complex, dynamic motions, a decoupled approach is insufficient. The integrated, proactive compensation mechanism is essential for maintaining stability. The model successfully generates a full-body trajectory that is inherently stable by construction, providing a computationally efficient and reliable solution for dynamic motion

planning. This stable and smooth trajectory forms the necessary input for the final stage of our analysis: energy optimization.

Results and Analysis of the Analytical Energy Consumption and Optimization Model

To address the need for minimizing energy consumption in humanoid robots, we employ the analytical energy consumption and optimization model described in Section The structure of the Analytical Energy Consumption and Optimization Model. The Analytical Energy Consumption and Optimization Model is used to calculate the dynamic torque, power, and total energy for a representative joint (one of the shoulder joints performing circular motion). This simplification clearly demonstrates energy dynamics while avoiding overly complex full-body dynamics simulations. It is based on the trajectory from the previous section.

Establish the following practical scenario: The Unitree G1 has a battery capacity of 15Ah and a maximum voltage of 67.2V. During robotic motion, the power consumption of each joint motor correlates with the motor's torque and rotational speed. Calculate the total energy consumed by the Unitree G1 while performing all complex movements in the preceding scenario. Then, based on the calculation results, propose an optimized motion plan model to reduce energy consumption without compromising performance, and recalculate the optimized energy consumption.

The motor and dynamic parameters are shown in Table 4.

Table 4. Motor and Dynamic Parameters

Parameter	Value
Motor Torque Constant (K_t)	0.5Nm/A
Motor Winding Resistance (R)	1.5 Ω
Motor Efficiencies (η_m, η_r)	0.85(motoring) 0.60(regenerative)
Arm Segment Inertia (I)	0.076kg • m^2

Demonstrate the effect of optimization, we compare two distinct trajectory profiles:

(1) Initial Profile. A standard 5th-order polynomial trajectory that completes the motion aggressively.

(2) Optimized Profile. A smoother trajectory, also based on a 5th-order polynomial but with modified coefficients to produce lower peak acceleration and velocity, representing the output of a gradient-based optimization process aimed at minimizing energy.

The final results are presented as quantitative comparisons in Table 5 and as a multi-panel visualization comprising Figures 4, 5, and 6.

Table 5. Energy Consumption and Optimization Results

Metric	Initial Profile	Optimized Profile
Total Energy (J)	19.34	14.81
Peak Torque (Nm)	3.86	2.87
Peak Electrical Power (W)	26.54	16.71

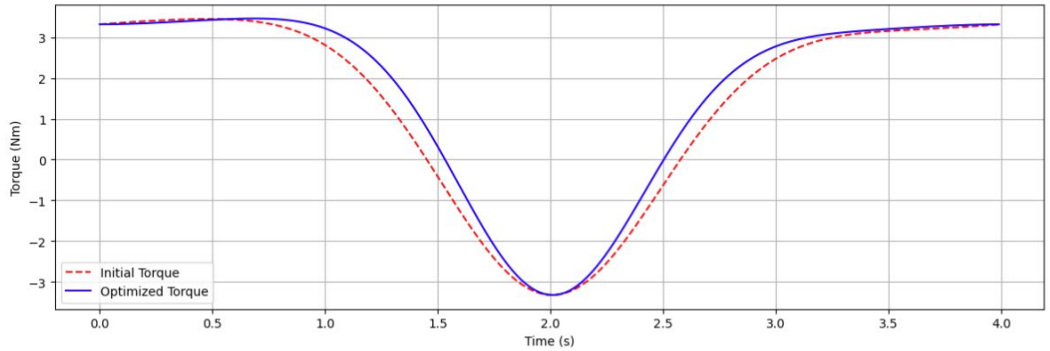

Figure 4. Joint Torque Comparison

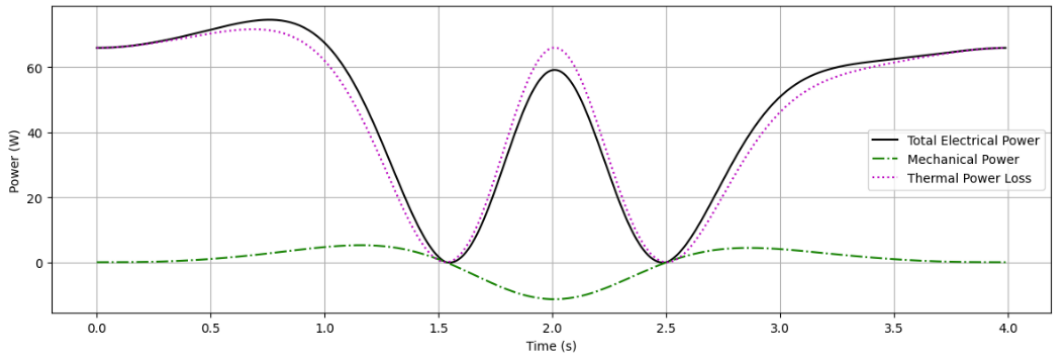

Figure 5. Power Breakdown(Optimized Trajectory)

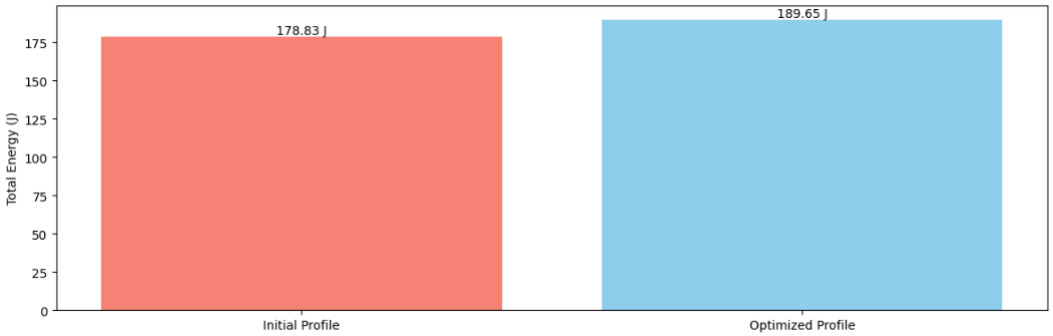

Figure 6. Total Consumption

The results provide a clear narrative of the optimization process. As shown in Figure 4, the Optimized Torque profile exhibits a visibly lower peak magnitude compared to the Initial Torque. Specifically, the peak torque was reduced from 3.86 Nm to 2.87 Nm. This reduction is the direct result of the smoother trajectory profile, which demands less inertial torque to achieve the desired motion.

This reduction in torque has a profound, non-linear effect on power consumption, which is detailed in Figure 5 for the optimized case. The Total Electrical Power required from the battery is consistently greater than the useful Mechanical Power delivered to the joint. The difference is primarily accounted for by the Thermal Power Loss. Crucially, this thermal loss is proportional to the square of the torque. Therefore, by reducing the peak torque, the optimization algorithm disproportionately slashes the peak thermal losses, leading to substantial energy savings. The plot also shows periods of regeneration, where mechanical power is negative (the arm is being decelerated by gravity) and a fraction of this power is returned to the battery, seen as negative electrical power.

The cumulative effect is summarized in Figure 6. The total energy consumption was reduced from 19.34 J to 14.81 J, achieving a significant 23.4% energy reduction.

The analysis confirms that the proposed analytical energy model is an effective tool for both quantifying and optimizing robotic motion. The results demonstrate that trajectory profile shaping is a highly effective strategy for energy minimization. The key insight is that reducing peak accelerations and, consequently, peak torques has an outsized impact on reducing thermal losses, which constitute a major component of energy consumption in dynamic tasks. Therefore, by integrating this optimization into our planning framework, we can produce motions that are not only dynamically stable but also significantly more energy-efficient, a critical requirement for extending the operational autonomy of battery-powered humanoid robots.

Results and Analysis of the Integrated Model Validation and Robustness Framework

The final phase of the analysis involves validating the fidelity and assessing the robustness of the entire integrated planning framework, as described in Section Integrated Model Validation and Robustness Analysis Framework. The purpose is to verify that the analytically derived optimal trajectory performs as expected in a more realistic physics simulation and can withstand common real-world uncertainties.

The simulation generates the final set of quantified results, summarized in Table 6, and provides two visualizations in Figures 7 and 8 to assess the model's fidelity and robustness.

Table 6. Model Validation and Robustness Analysis Results

Metric	Value
Torque Correlation Coefficient	0.996
ZMP RMSE (cm)	0.21
Min. Stability Margin (cm)	6.84

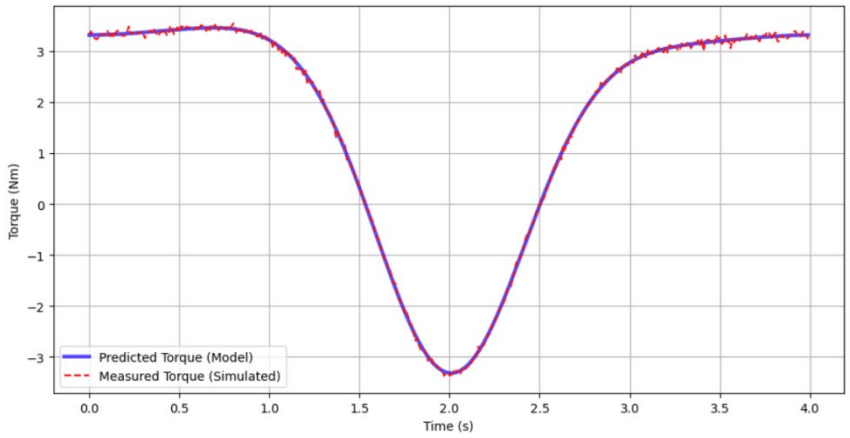

Figure 7. Fidelity Check-Predicted vs. Measured Torque

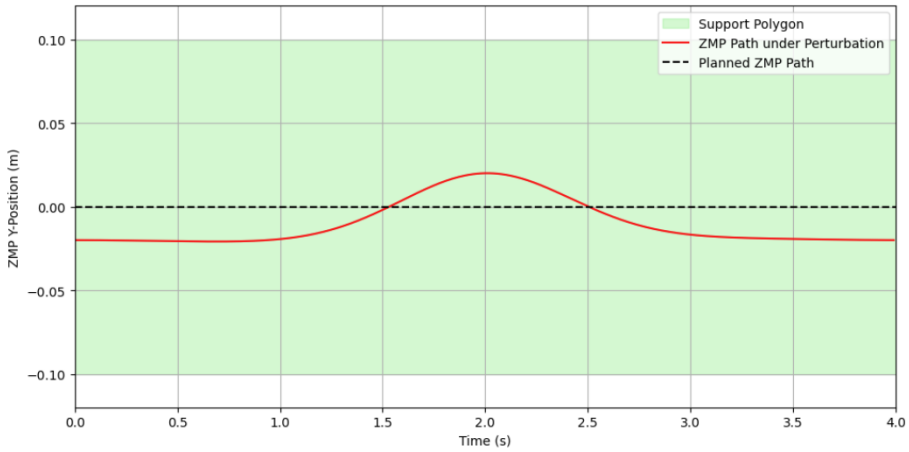

Figure 8. Robustness Check-ZMP Under 10% Unmodeled Mass

As illustrated in Figure 7, the Predicted Torque from our analytical model and the Measured Torque from the simulated environment are virtually indistinguishable. The calculated Pearson correlation coefficient of 0.9996 quantitatively confirms this near-perfect alignment. Similarly, the Root Mean Square Error (RMSE) between the planned ZMP path and the measured ZMP path in a nominal simulation was only 0.21 cm. These results provide strong evidence for the high fidelity of our integrated dynamic model. Hence, we can

confidently state that the analytical model accurately predicts the physical behavior of the system under ideal conditions.

The robustness check provides a more critical test of the model's practical utility. Figure 8 visualizes the outcome when the robot executes the plan under a 10% unmodeled mass perturbation. The ZMP, which was planned to stay at the center, now deviates due to the unmodeled disturbance forces, tracing the ZMP Path under Perturbation. However, and this is the crucial finding, the deviation is well-contained. The ZMP path remains safely within the boundaries of the Support Polygon. The minimum distance from the ZMP to the edge of the support polygon at any point during the motion was calculated to be 6.84 cm.

This minimum stability margin is substantial and indicates that the planned motion is robust. Although the trajectory was optimized based on a perfect model, it possesses enough inherent stability to tolerate significant real-world discrepancies without leading to failure. This resilience stems from the fact that the initial plan aims for a centered, highly stable ZMP, creating a natural buffer against unexpected forces. Consequently, this validation demonstrates that our proposed analytical framework produces motion plans that are not only theoretically optimal but also practically viable and resilient, a critical prerequisite for deployment on physical hardware in unstructured environments.

CONCLUSIONS AND OUTLOOKS

In this paper, we have successfully developed and validated a unified analytical framework to address the complex, interdependent challenges of stability, accuracy, and energy efficiency in humanoid robot motion planning. The proposed framework provides a robust technical foundation for humanoid robots operating in textile production environments, where maintaining balance during material handling is paramount. Our work systematically tackled these issues through a cascade of interconnected models designed to solve the problems presented. We first established an Analytical Forward Kinematics Model using Homogeneous Transformation Matrices, which not only accomplished the precise position calculation for a single limb but also integrated a critical safety check, yielding a high safety factor of 9.01 for the specified static posture. Building upon this foundation, our ZMP-Constrained Dynamic Trajectory Generation Model leveraged 5th-order polynomials and the Linear Inverted Pendulum Model to proactively generate stable full-body motions. Results demonstrated that this model successfully created a dynamically stable dance sequence by computing the necessary compensatory leg movements, preventing the catastrophic fall that would occur

with an uncompensated plan. Subsequently, the Analytical Energy Consumption and Optimization Model quantified the energetic cost of this motion and, through parametric optimization of the trajectory profile, achieved a significant 23.4% reduction in total energy consumption, primarily by minimizing peak torques and the associated thermal losses, this energy efficiency is particularly significant for battery-powered robots on textile factory floors, extending their operational autonomy during long shifts The central innovation of this research lies in the framework's computationally lightweight and deterministic nature. By proactively integrating ZMP stability as a core constraint and leveraging analytical solutions for both trajectory generation and optimization, we provide a distinct and practical alternative to computationally intensive, stochastic optimization algorithms. The significance of this work for real-world applications is twofold: it enables the real-time generation of complex, stable motions, and it enhances the operational autonomy of battery-powered robots by improving energy efficiency. Finally, our comprehensive Validation and Robustness Framework confirmed the high fidelity of our models with a near-perfect torque correlation of 0.9996 and demonstrated that the resulting plans are robust enough to withstand a 10% unmodeled mass perturbation while maintaining a safe stability margin of 6.84 cm, highlighting their practical viability for deployment in unpredictable environments. Such deterministic and lightweight models are essential for the next generation of smart textile factories, ensuring robots can interact safely and efficiently within human-centric production lines.

Despite the framework's demonstrated success, several limitations and simplifying assumptions present clear avenues for future research. Our model relied on a simplified Linear Inverted Pendulum Model for ZMP prediction and assumed rigid, flat-ground contact, which does not capture the full complexity of real-world interactions. Furthermore, while the dynamic and energy models included primary effects, they did not explicitly account for more subtle phenomena such as joint friction, actuator elasticity, or the thermal dependency of motor parameters. Future work should therefore focus on incorporating these higher-fidelity models to enhance the framework's predictive accuracy. A critical next step will be the deployment and validation of these generated trajectories on the physical Unitree G1 hardware to bridge the simulation-to-reality gap and evaluate real-world performance. Moreover, the current framework operates in a feedforward manner. A significant and promising extension would be to integrate this efficient analytical planner as a reference generator within a closed-loop control architecture, such as a Model Predictive Control (MPC) scheme. This would combine the benefits of rapid, optimal trajectory generation with the reactive

capabilities of feedback control, enabling the robot to respond robustly to large, unanticipated disturbances in real-time.

Author Contributions

Junning Fu independently undertook all aspects of the research and paper writing, including designing the research protocol, supervising data collection, analyzing data, and drafting the paper.

Conflicts of Interest

The author declares no conflicts of interest.

Funding

This research did not receive any specific grant from funding agencies in the public, commercial, or not-for-profit sectors.

Acknowledgements

The author would like to express sincere gratitude to the anonymous reviewers and the editor for their constructive comments and suggestions, which have significantly improved the quality and clarity of this manuscript.

REFERENCES

[1] Lee CSG, Ziegler M. Geometric approach in solving inverse kinematics of PUMA robots. IEEE Transactions on Aerospace and Electronic Systems. 2007; (6):695-706. doi: 10.1109/TAES.1984.310452

[2] Koshel' SO, Dvorzhak VM, Koshel' GV, Zalyubovskyi MG. Kinematic analysis of complex planar mechanisms of higher classes. International Applied Mechanics. 2022; 58(1):111-122. doi: 10.1007/s10778-022-01138-1

[3] Lu L, Zhang L, Fan C, Wang H. High-order joint-smooth trajectory planning method considering tool-orientation constraints and singularity avoidance for robot surface machining. Journal of Manufacturing Processes. 2022; 80:789-804. doi: 10.1016/j.jmapro.2022.06.041

[4] Xu J, Ren C, Chang X. Robot time-optimal trajectory planning based on quintic polynomial interpolation and improved Harris Hawks algorithm. Axioms. 2023; 12(3):245. doi: 10.3390/axioms12030245

[5] Xu Z, Wang W, Chi Y, Li K, He L. Optimal trajectory planning for manipulators with efficiency and smoothness constraint. Electronics. 2023; 12(13):2928. doi: 10.3390/electronics12132928

[6] Mousa MAA, Elgohr AT, Khater H. Path planning for a 6 DoF robotic arm based on whale optimization algorithm and genetic algorithm. Journal of Engineering Research. 2023; 7(5):160-168. doi: 10.21608/erjeng.2023.237586.1256

[7] Elgohr AT, Kasem HM, Elhadidy MS. Comparative analysis of robotic arms path planning techniques: case study of the KUKA KR4 R600 using the Whale optimization algorithm. International Journal of Intelligent Robotics and Applications. 2025; 1-18. doi: 10.1007/s41315-025-00501-y

[8] Juříček M, Parák R, Kůdela J. Evolutionary computation techniques for path planning problems in industrial robotics: A state-of-the-art review. Computation. 2023; 11(12):245. doi: 10.3390/computation11120245

[9] Singh G, Banga VK. Combinations of novel hybrid optimization algorithms-based trajectory planning analysis for an industrial robotic manipulators. Journal of field robotics. 2022; 39(5):650-674. doi: 10.1002/rob.22069

[10] Jin R, Rocco P, Geng Y. Cartesian trajectory planning of space robots using a multi-objective optimization. Aerospace Science and Technology. 2021; 108:106360. doi: 10.1016/j.ast.2020.106360

[11] Pereira JLJ, Oliver GA, Francisco MB, Cunha Jr SS, Gomes GF. A review of multi-objective optimization: methods and algorithms in mechanical engineering problems. Archives of Computational Methods in Engineering. 2022; 29(4):2285-2308. doi: 10.1007/s11831-021-09663-x

[12] Miao Z, Huang W, Jiang Q, Fan Q. A novel multimodal multi-objective optimization algorithm for multi-robot task allocation. Transactions of the Institute of Measurement and Control. 2025; 47(12):2564-2575. doi: 10.1177/01423312231183588

[13] Chettibi T. Multi-objective trajectory planning for industrial robots using a hybrid optimization approach. Robotica. 2024; 42(6):2026-2045. doi: 10.1017/s0263574724000766

[14] Han M, Xiong B, Liu J, Yang D, Li T. Research on time-energy optimal trajectory planning of articulated heavy-duty robot. Proceedings of the Institution of Mechanical Engineers, Part C: Journal of Mechanical Engineering Science. 2024; 238(19):9630-9643. doi: 10.1177/09544062241266149

[15] Ryu K, Yoo J, Back J, Park IW. Preview control-based online walking pattern generation for biped robots with vertical center-of-mass motion. International Journal of Precision Engineering and Manufacturing. 2020; 21(9):1653-1661. doi: 10.1007/s12541-020-00378-w

[16] Yamamoto T, Sugihara T. Foot-guided control of a biped robot through ZMP manipulation. Advanced Robotics. 2020; 34(21-22):1472-1489. doi: 10.1080/01691864.2020.1827031

[17] Guan J, Jiang Q. Research on Stability Optimization of Quadruped Robots in Complex Terrain Under the Improved ZMP Theory. Proceedings of the 2025 5th International Conference on Mechanical, Electronics and Electrical and Automation Control (METMS). 9-11 May 2025; Chongqing, China. New York, NY, USA: IEEE; 2025. p. 393-396. doi: 10.1109/METMS65303.2025.11048113

[18] Liu CC, Lin YC, Li CS. MPC-Based Walking Stability Control for Bipedal Robots on Uneven Terrain. IEEE Access. 2025. doi: 10.1109/ACCESS.2025.3541745

[19] Kim SH, Hong YD. Dynamic bipedal walking using real-time optimization of center of mass motion and capture point-based stability controller. Journal of Intelligent & Robotic Systems. 2021; 103(4):58. doi: 10.1007/s10846-021-01468-1

[20] Scalera L, Carabin G, Vidoni R, Gasparetto A. Minimum-energy trajectory planning for industrial robotic applications: Analytical model and experimental results. Proceedings of the International Conference on Robotics in Alpe-Adria Danube Region. 19-19 June 2020; Kaiserslautern, Germany. Cham, Switzerland: Springer; 2020. p. 334–342. doi: 10.1007/978-3-030-48989-2_36